Atomic-Scale Manipulation of Single-Polaron in a Two-dimensional Semiconductor

Huiru Liu[1,3†], Aolei Wang [2†], Ping Zhang[1,3], Chen Ma[1,3], Caiyun Chen[1,3], Zijia Liu[1,3],

Yiqi Zhang[1,3], Baojie Feng[1,3], Peng Cheng[1,3], Jin Zhao [2*], Lan Chen[1,3,4*], Kehui Wu[1,3,4*]

[1] *Institute of Physics, Chinese Academy of Sciences, Beijing 100190, China*

Ben Safvati
11/14/22

Background: Polaron Quasiparticle

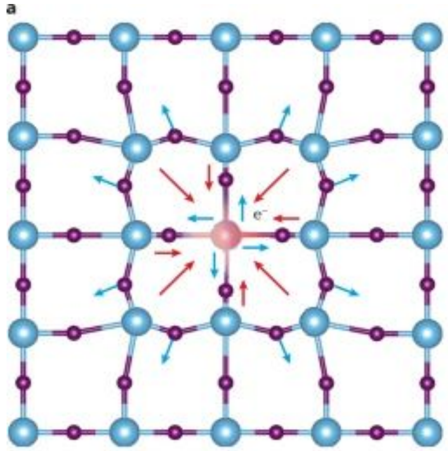

- Composite quasiparticle made of an **electronic carrier plus the altered atomic motion induced by it's presence**.
- Coulomb force from excess charge distorts ions in lattice, charge becomes "**self-trapped**" in potential well created by lattice displacement.
- Displaced ions are polarized by excess charge, extent of polarization cloud determines polaron size, electronic characteristics.

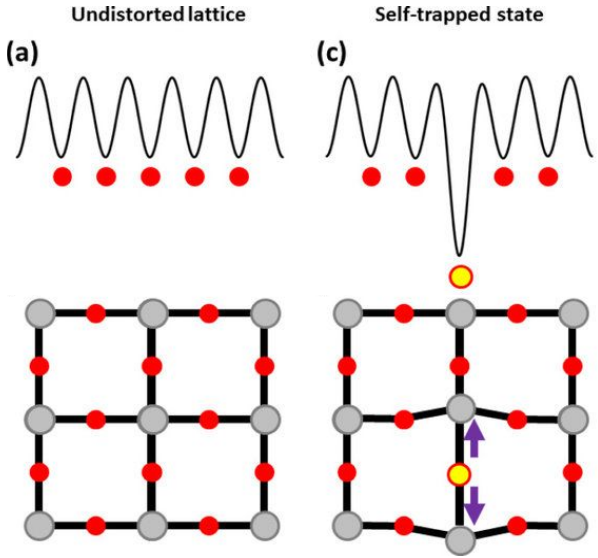

Small 'Holstein' polarons

$$\boldsymbol{H} = \sum_{\mathbf{k}} \varepsilon_{\mathbf{k}} \hat{c}_{\mathbf{k}}^{\dagger} \hat{c}_{\mathbf{k}} + \hbar\omega_0 \sum_{\mathbf{q}} \hat{a}_{\mathbf{q}}^{\dagger} \hat{a}_{\mathbf{q}} + \frac{g}{\sqrt{N}} \sum_{\mathbf{k},\mathbf{q}} \hat{c}_{\mathbf{k}+\mathbf{q}}^{\dagger} \hat{c}_{\mathbf{k}} (\hat{a}_{\mathbf{q}} + \hat{a}_{-\mathbf{q}}^{\dagger})$$

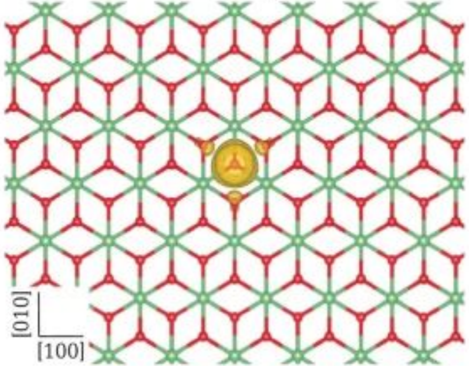

- Short-range electron–phonon interaction
- Polaron radius ≈ lattice parameter
- Narrow mid-gap electronic state (≈ 1 eV below E_F)
- Incoherent motion (phonon assisted)
- Thermally activated hopping mobility ≪ 1 $cm^2 V^{-1} s^{-1}$
- Mobility increasing with temperature

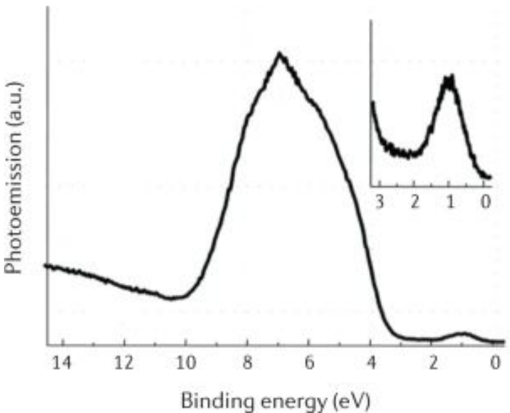

Large 'Fröhlich' polarons

$$\boldsymbol{H} = \sum_{\mathbf{k}} \varepsilon_{\mathbf{k}} \hat{c}_{\mathbf{k}}^{\dagger} \hat{c}_{\mathbf{k}} + \hbar\omega_0 \sum_{\mathbf{q}} \hat{a}_{\mathbf{q}}^{\dagger} \hat{a}_{\mathbf{q}} + \sum_{\mathbf{k},\mathbf{q}} V(\mathbf{q}) \hat{c}_{\mathbf{k}+\mathbf{q}}^{\dagger} \hat{c}_{\mathbf{k}} (\hat{a}_{\mathbf{q}} + \hat{a}_{-\mathbf{q}}^{\dagger})$$

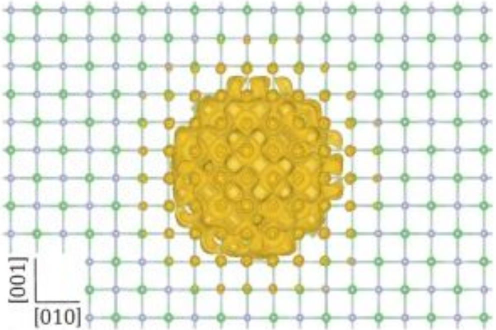

- Long-range electron–phonon interaction
- Polaron radius ≫ lattice parameter
- Shallow electronic state (≈ 10 meV below E_F)
- Coherent motion
- Free carrier mobility ≫ 1 $cm^2 V^{-1} s^{-1}$
- Mobility decreasing with temperature

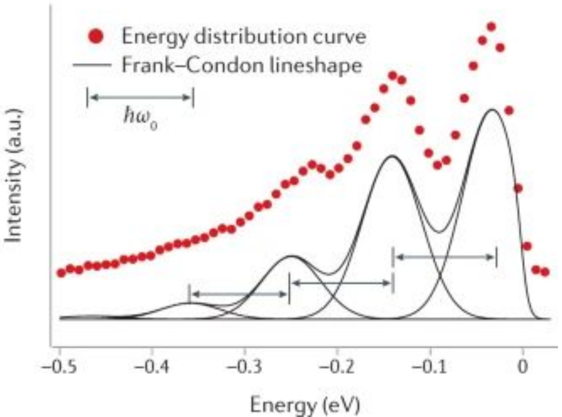

Background: Polaron Quasiparticle

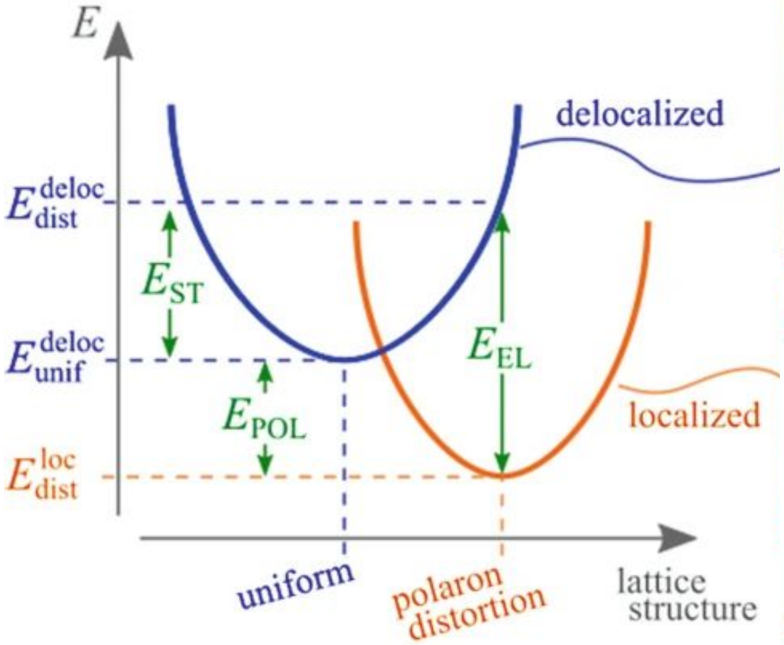

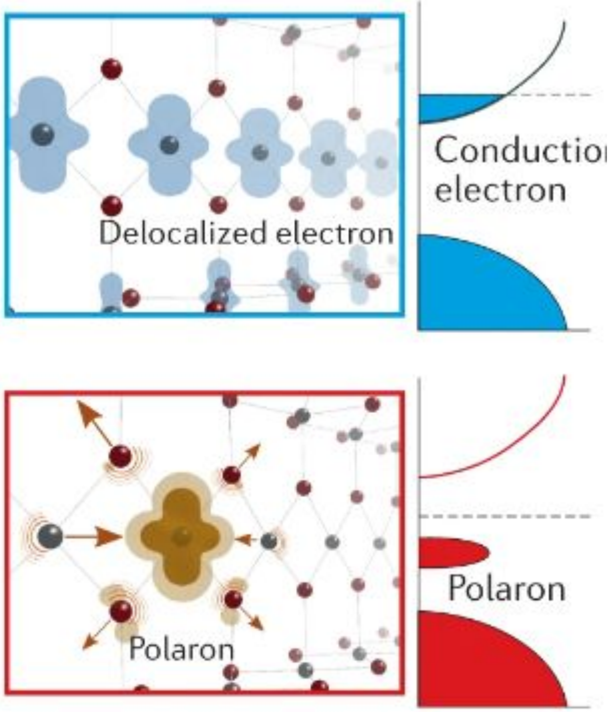

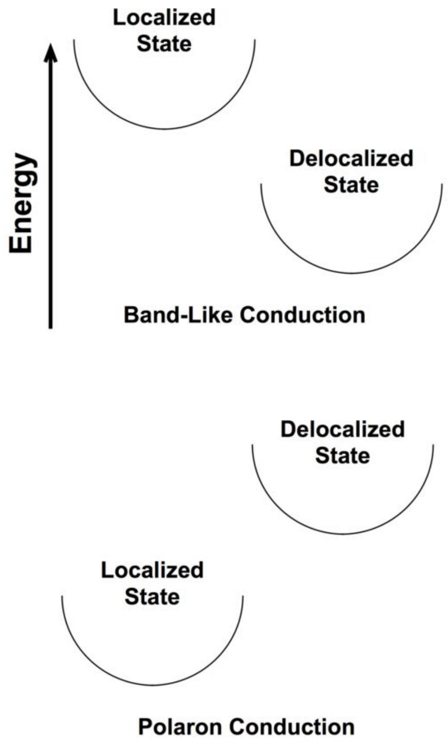

Background: Polaron Quasiparticle

Year	Material	Polaron source	Technique	Detected polaron
1963 (ref.[15])	UO_2	Oxidation	Conductivity measurements	Small
1964 (ref.[314])	$SrTiO_3$	O vacancies, Nb	Conductivity and Seebeck	Large
1970 (ref.[206])	ZnS, ZnSe	Photoexcitation	Raman spectroscopy	Large
1976 (ref.[315])	EuO	O vacancies	Optical absorption	Small
1977 (ref.[202])	CeO_2	O vacancies	Conductivity and Seebeck	Small
1987 (ref.[316])	Conjugated polymers	Photoexcitation	Photoluminescence	Small
1994 (ref.[222])	$BaTiO_3$	Nb doping	EPR	Small
1996 (ref.[27])	$LaMnO_3$	Sr doping	Neutron scattering	Small
2001 (ref.[225])	$LaMnO_3$	Ca doping	NMR and muon spin rotation	Small
2005 (ref.[227])	CeO_2	O vacancies	STM	Small
2007 (ref.[226])	$PrMnO_3$	Ca doping	TEM	Small (Zener)
2007 (ref.[200])	a-TiO_2 and r-TiO_2	Nb doping	Conductivity and optical measurements	Large (a), small (r)
2008 (ref.[196])	r-TiO_2	O vacancies	Resonant photoelectron diffraction	Small
2010 (ref.[56])	$SrTiO_3$	Nb doping	Optical conductivity	Large
2013 (ref.[51])	r-TiO_2	O vacancies	EPR	Small
2013 (ref.[48])	a-TiO_2	O vacancies	ARPES	Large
2014 (ref.[46])	r-TiO_2	O vacancies	STM and STS	Small
2015 (ref.[55])	r-TiO_2	UV/H adatom	Infrared spectroscopy	Small
2016 (ref.[317])	$LiNbO_3$	Photoexcited	Infrared spectroscopy	Small
2017 (ref.[30])	$CH_3NH_3PbBr_3$ and $CsPbBr_3$	Photoexcited	TR-OKE	Large
2017 (ref.[219])	a-TiO_2	Photoexcited	TR-XAS	Large
2020 (ref.[83])	Fe_2O_3	Photoexcitation	RIXS	Small

Growth and characterization of $CoCl_2$ on HOPG

- $CoCl_2$ monolayers grown with MBE in UHV at room temperature.
  - HOPG cleaved in air and loaded beforehand.
  - STM/MBE hybrid system keeps sample in UHV.

- Dendritic growth of monolayer off HOPG step edges.

- Observation of moire patterns on surface at some locations, implies substrate can significantly affect monolayer properties.

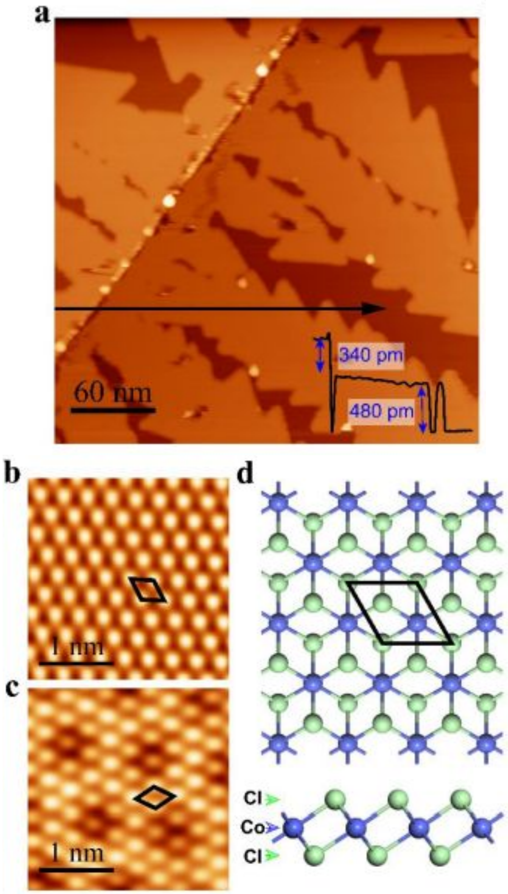

STM/S characterizations of CoCl2 on HOPG

- STS shows ~1.7 eV semiconducting gap, Fermi level ~0.4 eV below CBE shows sample is e-doped.

- HOPG linear DOS seen inside band gap.

- Calculated band structure has 4.1 eV gap, authors believe HOPG has strong influence.
    - Theoretical DOS including substrate shows several mid-gap states.

e

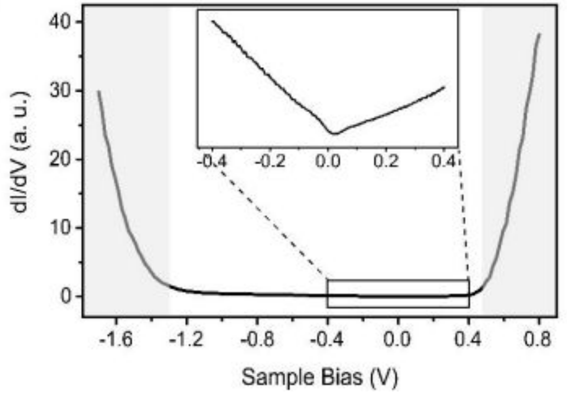

f

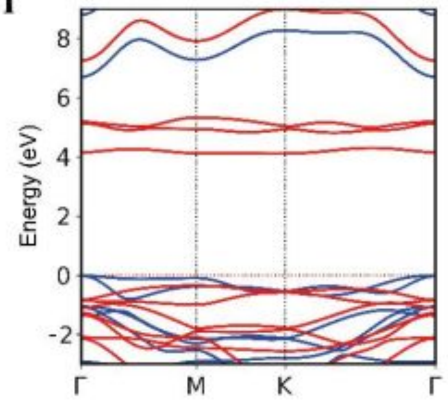

Manipulation of single polarons

- "Highly reproducible" hysteresis effect with STM bias sweeps.
- Positive sweep peak corresponds to electron injection, ring feature appears after.
    - Negative sweep dip erases ring feature.
- At constant bias and no feedback, can observe current jumps corresponding to different processes by applying 1 sec pulses.

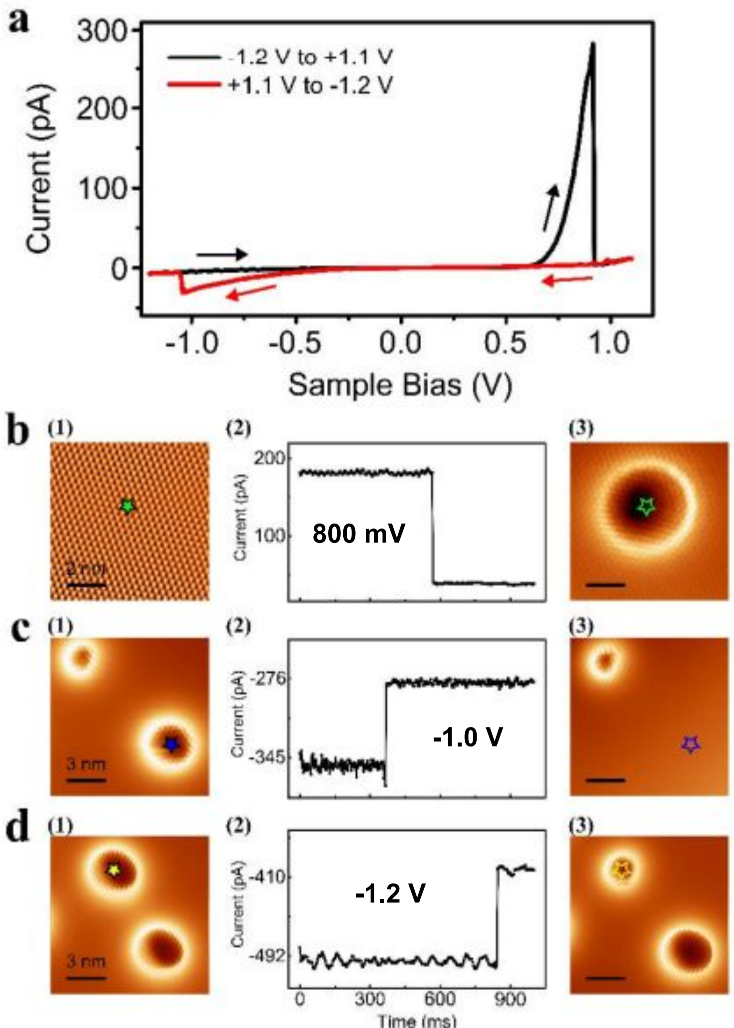

Manipulation of single polarons

- “Highly reproducible” hysteresis effect with STM bias sweeps.
- Positive sweep peak corresponds to electron injection, ring feature appears after.
    - Negative sweep dip erases ring feature.
- At constant bias and no feedback, can observe current jumps corresponding to different processes.

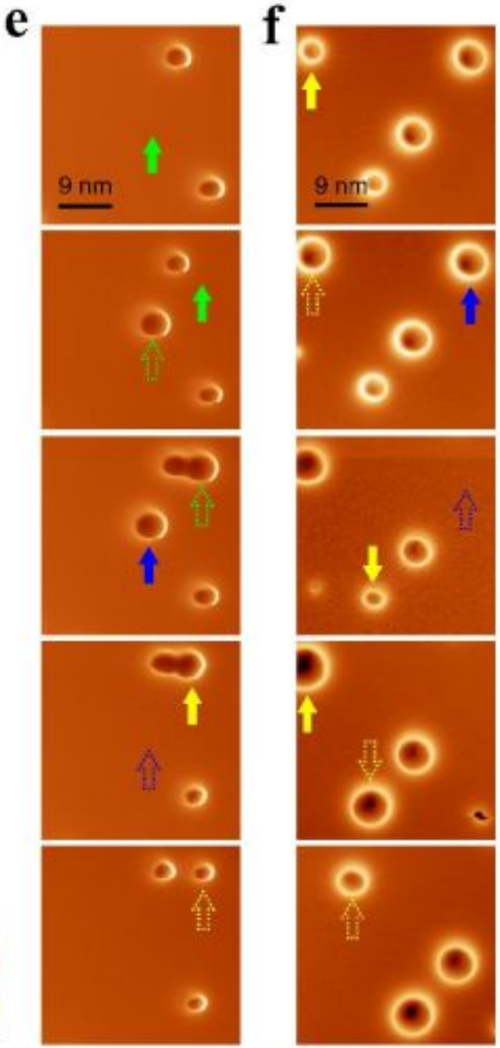

Bias-dependent Polaron Features

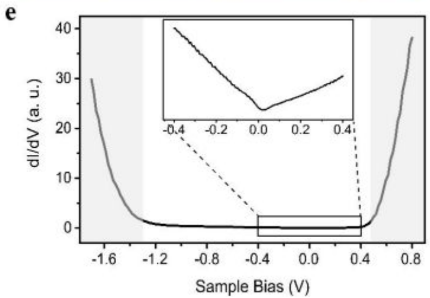

Topo in CB:
- Dominated by polaron feature.
- Dark disk is result of band bending.

Topo in band gap:
- Shows no lattice defect creating this feature.

Shrinking disk with increasing bias more evidence of Conduction band upward bending.

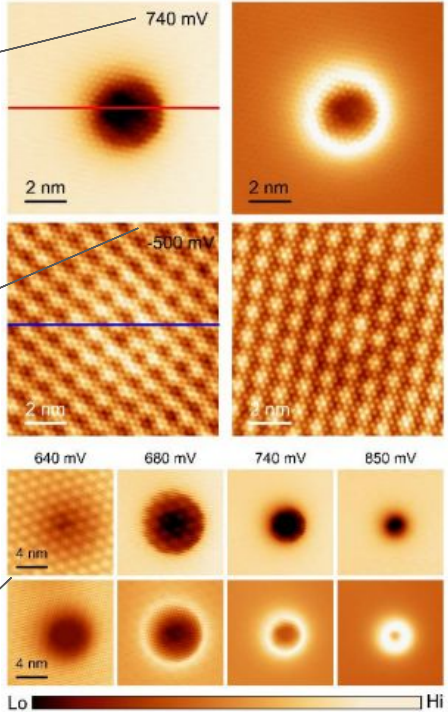

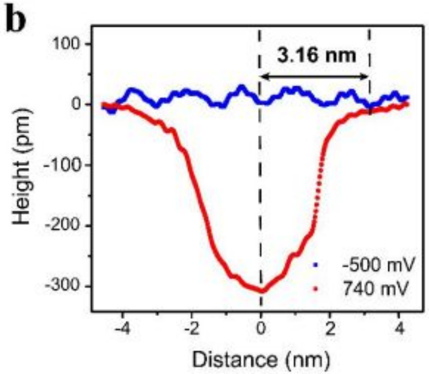

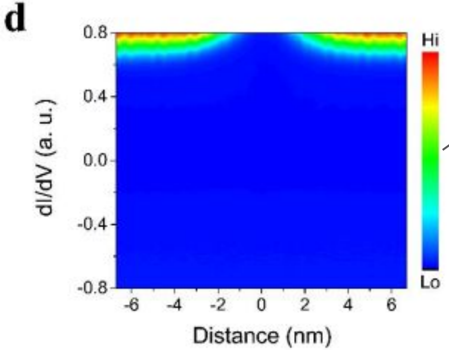

Band bending color map: incorrect labels?

Two types of polarons in CoCl2

- Two types of polarons observed depending on location of electron injection.
  - Type-I: centered on upper Cl site, larger.
  - Type-II: centered on Co site, smaller.

- In their experiments, Type-I was more common, believed to be more energetically stable.

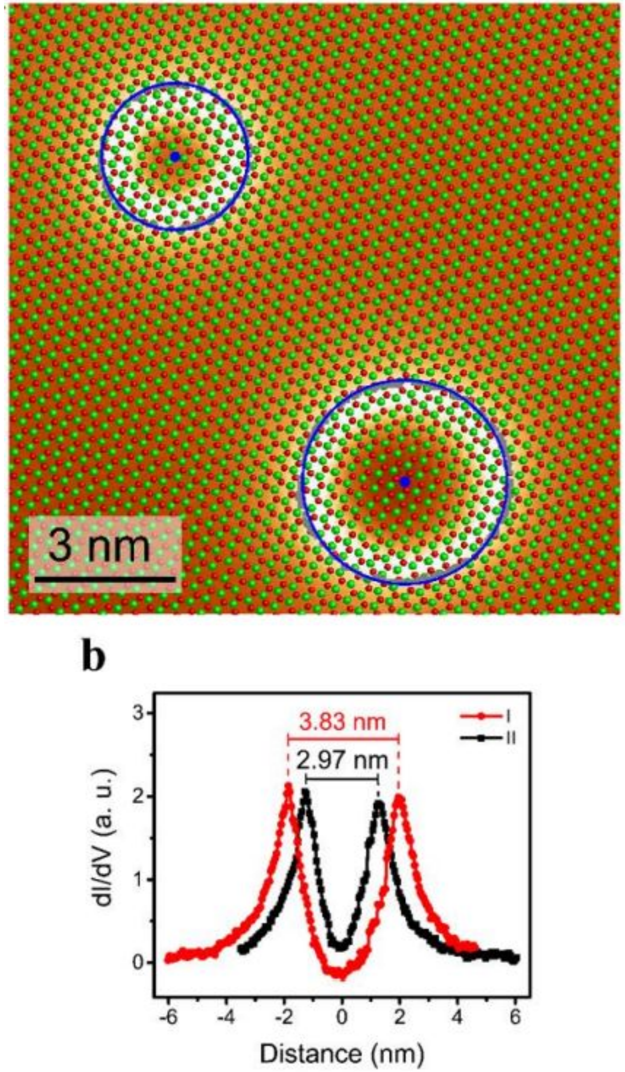

Theoretical modelling of polarons

- DFT predicts two stable polaron configurations with one extra electron in CB.
    - Lattice displacements are short-ranged, beyond limit of STM spatial resolution.

- Type-I polaron charge density is spread across three neighboring Co atoms, Type-II density concentrated at single Co.
    - Agrees with larger disk size for Type-I.

- Predicted type-I polaron binding energy is larger, evidence of greater stability.

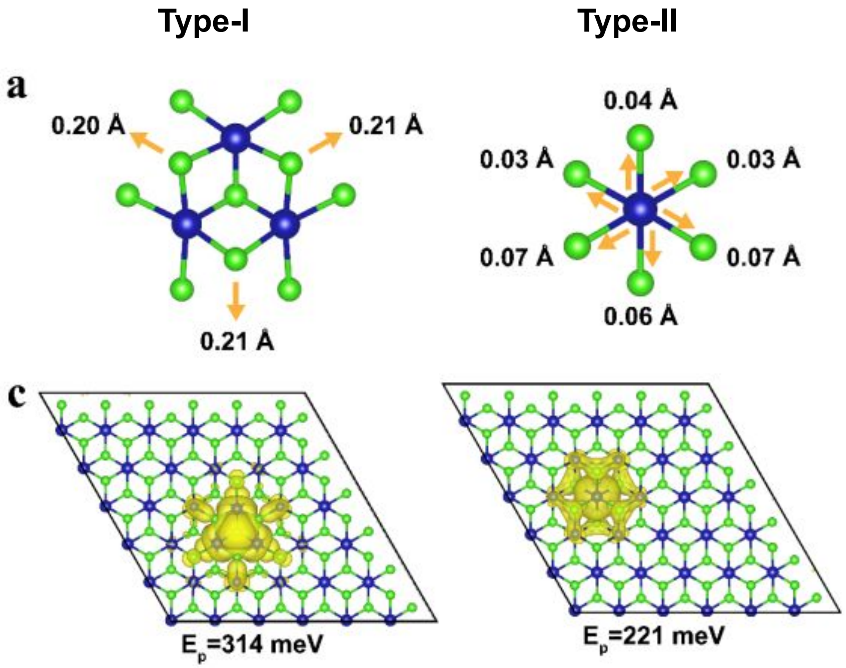

Theoretical modelling of polarons

- Theoretical spin-resolved DOS predicts both polarons are spin-polarized.
- Mid-gap states appear as peak (type-I) or peaks (type-II) just below Fermi level.
- Simulated electrostatic potentials agree with observed polaron sizes.

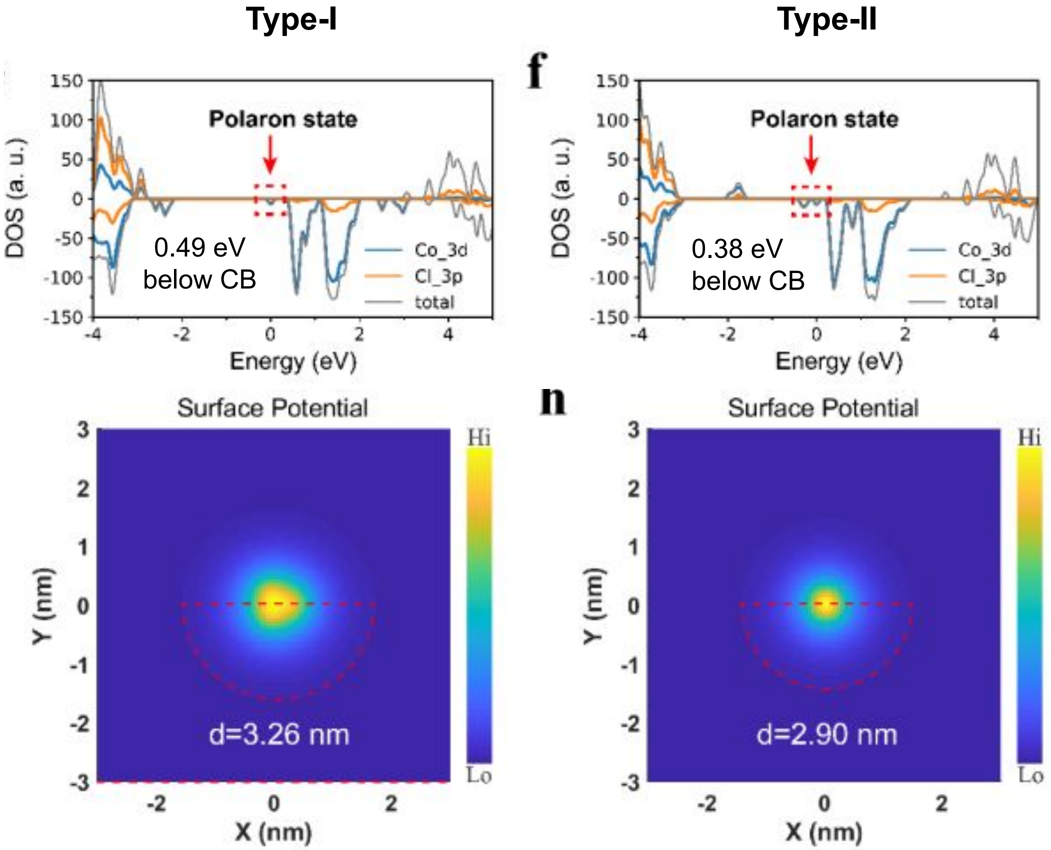

Manipulation mechanism of polaron

- Writing process is based on electron injection into CB of CoCl2 monolayer.

- DFT predicts CB is 600 meV above Fermi level, yet experimental bias threshold is 858 meV.

- Explanation is that voltage drops across CoCl2 monolayer in addition to tip-sample, decreasing overall bias at the sample surface.

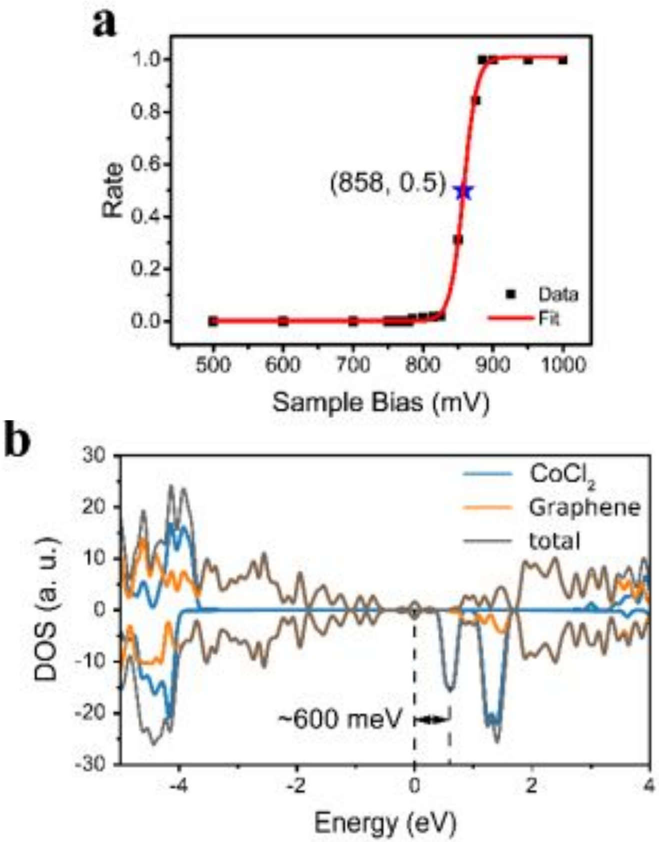

Conclusions/Relevance

- Polarons were found on a 2D semiconductor grown on HOPG, and they were shown to be simple to create and manipulate.
- Opportunities to study atomic-scale polaronics, create nanoscale structures out of polarons (polaronic lattices).
- Polarons act as spin-polarized localized electrons, platform for 2D magnetism.
- Study role of polarons in superconductivity with SC tip.